Nonlinear behaviour of groundwater-surface water exchange flux

M. Tripathi[1,2], P. K. Yadav[3], M. Walther[4,5], R. Liedl[3], B. R. Chahar[1,] and P. Dietrich[2]

[1]Indian Institute of Technology, Department of Civil Engineering, Delhi, India

[2]Helmholtz Centre for Environmental Research GmbH – UFZ, Department of Monitoring and Exploration Technology, Leipzig, Germany

[3]Technische Universität Dresden, Faculty of Environmental Sciences, Department of Hydrosciences, Institute for Groundwater Management, Professorship of Groundwater Management

[4]Technische Universität Dresden, Faculty of Environmental Sciences, Department of Hydrosciences, Institute for Groundwater Management, Professorship for Contaminant Hydrology

[5]Helmholtz Centre for Environmental Research GmbH – UFZ, Department of Environmental Informatics, Leipzig, Germany

Corresponding author: Moulshree Tripathi (t.moulshree@gmail.com)

Key Points:

1. Developed an analytical approach to quantify GW-SW exchanging flux and to highlight the significance of underlying aquifer.
2. The exchanging flux follows a nonlinear behaviour when aquifer properties are part of flux quantification.
3. Provided a simpler approach to determine streambed specific conductance.

Abstract

Understanding of the groundwater (GW)-surface water (SW) interaction is essential for the both qualitative and quantitative determination of the exchanging flux between them. The commonly used conductance-based approach, which linearly relates the flux with the streambed conductance, avoids the inclusion of aquifer properties in the flux quantification. In this approach, aquifer properties are solely represented by a hydraulic head below the streambed. Applying an analytical approach to a superimposed GW-SW system, this work finds that the exchanging flux rather follows a nonlinear behaviour when aquifer properties are part of flux quantification. The developed approach is found to match the numerical results obtained from synthetic data. The study further provides approaches for simpler quantification of geometrical and hydraulic properties of the streambed and the aquifer.

Keywords: Stream-aquifer interaction, parameter estimation, analytical approach, numerical modelling

1 Introduction

The interactions between groundwater (GW) and the surface water (SW), the two major components of the hydrological cycle, have great significance for the nutrient transport (Bencala, 2005), for maintaining riparian ecology (Boulton et al., 1998) and several other ecological functions (Brunner et al., 2017). Compared to initial studies, these two components are now widely recognised and researched as a single hydrological unit (Malard et al., 2002; McLachlan et al., 2017). Its high ecological significance has increased the interest in GW-SW interaction modelling (Boano et al., 2014; Brunner et al., 2017). It is now well established that the interactions are mostly controlled by the two major components of the stream-aquifer system – a) streambed and b) aquifer beneath the streambed (Alzraiee et al., 2017; Cardenas et al., 2004).

A streambed with respect to GW-SW interactions can be defined as an interface between the stream and the aquifer. Studies such as Frei et al., (2009), Kalbus et al., (2009), Vogt et al., (2010) suggest that depending on the scale of the study, the hydrological properties (hydraulic conductivity, porosity etc.), the geometrical properties (streambed width and thickness) and the bedforms, of the streambed governs the GW-SW exchange. Among these, the hydraulic

conductivity of the streambed (K_r) has been suggested (e.g. Tang et al., 2017) to be the most crucial parameter and a thorough knowledge of its spatial distribution is required for appropriate estimation of GW-SW flux. However, the investigation of the spatial distribution K_r is a challenging task, largely because of complexities of geological structures (Benoit et al., 2019). The streambed thickness is another important parameter that significantly influences this exchange. Field estimation of the streambed thickness is extremely difficult and it is generally considered amongst a calibrating quantity in the modeling studies (e.g. CRIV in RIV Package, MODFLOW, McDonald & Harbaugh, 1988).

The hydraulic conductivity of the aquifer (K_a), beneath the streambed, and its thickness are the two significant quantities that guide the interactions through the streambed (Kalbus et al., 2009). However, only very few modelling studies have tried to incorporate and model the influence of aquifer beneath the streambed (e.g., Cousquer et al., 2017; Ghysels et al., 2019) to quantify GW-SW interaction. The clear understanding of the overall nature of GW-SW interactions requires a thorough understanding of the processes and reliable estimation of the flux across the stream bed.

Numerical modelling approaches (e.g., RIV package of MODFLOW) utilising the linear relationship between the flux and head-gradient, a so-called conductance-based approach, is most commonly used for estimating GW-SW flux (e.g. Brunner et al., 2010; Ghysels et al., 2019; Gooseff et al., 2006). The linear relation provides a possibility of infinitely increasing flux, which may not always be practical.

In general, research works such as Brunner et al., (2010) considers the head difference between the stream head and the head in the cell (or in the underlying aquifer) in which the stream is modelled for quantifying the exchanges. As per this approach if the head in the aquifer ($h_{aquifer}$) falls below the streambed bottom, the head in streambed bottom (h_{rbot}) replaces $h_{aquifer}$ (e.g. RIV Package of MODFLOW). In practical cases, the streambed thickness may vary in a range from few millimetres to few centimetres, and can significantly influence the head drop and the vertical hydraulic gradient below the streambed. This leads to high uncertainties in the determination of the streambed bottom or the thickness of colmation layer, and hence

increases the challenge with accurate quantification of h_{rbot}. To alleviate the challenge, this study proposes that $h_{aquifer}$ be measured at a certain distance from the stream.

The conductance of the streambed is a lumped parameter, consisting of the hydraulic as well as the geometrical properties of the streambed (e.g., Ghysels et al., 2019). The uncertainties involved in the quantification of the hydraulic conductivity, the width of the stream and the streambed thickness are extensively documented in works of Brunner et al., (2010), Ghysels et al., (2019). In addition, the accurate determination of hydraulic gradient in or below the streambed also poses a significant challenge, as the gradients may vary over a very short distance (Cremeans & Devlin, 2017).

Utilising mathematical approaches (analytical and numerical) this paper aims to study the contribution of the stream and the underlying aquifer on the flux and the resulting behaviour of the exchanging flux. The study develops an analytical approach to quantify the GW-SW flux from a 2D, two-component (streambed-aquifer) model setup. The behaviour of the flux through the developed analytical model is compared with a general numerical model using synthetic data. Finally, the significance of the developed approach and the properties of the underlying aquifer is highlighted.

2. Approach

The approach conceptualises a system with two components, a stream and an aquifer separated by a colmation layer (see Fig. 1). There exist two flows: (1) the vertical flow through the streambed and (2) the horizontal groundwater flow. The combined stream-aquifer system of this study represents the superposition of the horizontal groundwater flow and the vertical flow through the streambed. The superimposed system provides the flexibility to compute the flux through streambed separately and then incorporate the effect of it to the groundwater flow. For the conceptual development, we assume flow only through the streambed, i.e. without the groundwater flow. Further, the system is assumed to be homogenous, saturated and in a steady-state. In this setup (Fig. 1), K_a $[L/T]$, W_a $[L]$, and t_a $[L]$ define the aquifer properties, representing the hydraulic conductivity, width and thickness, respectively. Q_r [L^2/T] is the flux through the streambed. Q_{rr} [L^2/T] and Q_{rl} [L^2/T] are the integrated fluxes at the aquifer boundary, involving stream infiltration on the right and the left side, respectively. D $[L]$

corresponds to the distance from streambed to the aquifer side boundary, which is identical for both boundaries. The setup assumes that the head at the stream aquifer interface (h_{int}) remains constant along the entire width of the streambed. h_a is the head measured in the aquifer at distance D from the streambed and remains equal and constant on both the sides of the aquifer. This condition implies that the stream is the only source of water.

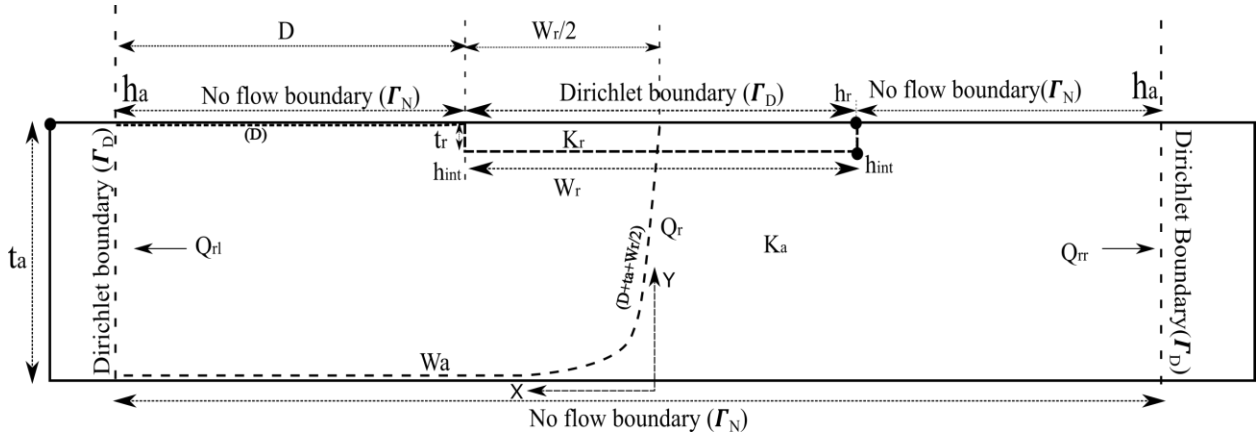

Figure 1: The conceptual model setup. The setup describes the geometrical and hydraulic properties of the system. It is a symmetrical system where fluxes are distributed equally on both the aquifer edges. $(D + t_a + W_r/2)$ and (D) represents the schematic shortest and longest streamlines for the model setup.

Based on the conductance concept (e.g. Ghysels et al., 2019), the GW-SW flux (Q [L^2/T]) per unit length of the stream is

$$Q = C\left(h_r - h_{aquifer}\right) \tag{1}$$

where h_r and $h_{aquifer}$ are the heads at the stream and the aquifer below the stream, respectively and $C\,[L/T]$ is the streambed conductance, which can be expressed as $C = (K_r\, W_r)/t_r$, in which, $K_r\,[L/T]$, $W_r\,[L]$, and $t_r\,[L]$ are the streambed hydraulic conductivity, width and thickness, respectively. The total flux through the streambed in this symmetric system is the sum of fluxes calculated at each aquifer boundary. When the flow equations are applied to each component individually, the expression for flux through the streambed (Q_r), a vertical flux from higher head h_r to lower the head h_{int} is

$$Q_r = K_r W_r \left(\frac{h_r - h_{int}}{t_r}\right) \quad (2)$$

Correspondingly, the flux ($Q_{rl}\ and\ Q_{rr}$) at either aquifer boundary can be expressed as the horizontal flux through the aquifer occurring due to the head gradient between the streambed bottom and the respective edge of the domain leading to

$$K_a t_a \left(\frac{h_{int} - h_a}{D + t_a + W_r/2}\right) < Q_{rl} < K_a t_a \left(\frac{h_{int} - h_a}{D}\right) \quad (3)$$

where the lower and the upper limits of the flux (at the left boundary in eq. 3) depends on the minimum (D) and maximum ($D + t_a + W_r/2$) distances for the gradient calculation, respectively. These distances are defined by the shortest and the longest streamline in the system (see Fig. 1). Eq. (3) thus incorporates both extremes of Q_{rl}. The symmetry of the setup will lead to identical expression as eq. (3) for Q_{rr}. Subsequent expressions will inherit the same ranges of fluxes as defined by eq (3).

As stated in the introductory section, h_{int} is subject to several challenges associated with its quantification, and hence we intend to replace it. From eq. (2) h_{int} can be obtained as

$$h_{int} = h_r - \frac{Q_r t_r}{K_r W_r} \quad (4)$$

Replacing h_{int} in eq. (3) from eq. (4) results to the following expression for flux at the aquifer boundary

$$K_a t_a \left(\frac{(h_r - Q_r t_r / K_r W_r) - h_a}{D + t_a + W_r/2}\right) < Q_{rl} < K_a t_a \left(\frac{h_r - Q_r t_r / K_r W_r - h_a}{D}\right) \quad (5)$$

which can be rearranged as

$$\frac{Q_{rl} D}{K_a t_a} + \frac{Q_r t_r}{K_r W_r} < h_r - h_a < \frac{Q_{rl}(D + t_a + W_r/2)}{K_a t_a} + \frac{Q_r t_r}{K_r W_r} \quad (6)$$

The symmetry of the setup and the constant head boundaries at the aquifer distributes the infiltrating stream flux equally to the edge of the aquifer. Therefore, the flux at the left and the right boundary will be

$$Q_{rl} = Q_r/2 \quad (7a)$$

$$Q_{rr} = -Q_r/2 \quad (7b)$$

The negative sign in eq. (7b) represents the opposite direction of the flow. Substituting Q_{rl} from eq. (7a) in eq. (6) and solving for Q_r we get

$$\frac{\Delta h}{\frac{(D+W_r/2+t_a)}{2K_a t_a}+\frac{t_r}{K_r W_r}} < Q_r < \frac{\Delta h}{\frac{D}{2K_a t_a}+\frac{t_r}{K_r W_r}} \tag{8}$$

Eq. (8) relates exchange flux with the hydraulic and geometrical properties of the streambed and the aquifer below it. Now, introducing the term specific conductance, C_r as

$$K_r/t_r = C_r \tag{9}$$

Unlike in eq. (1), the specific conductance in eq. (8), groups the parameters K_r and t_r, which generally are not quantified directly and, excludes W_r, which is easily determined. After some rearrangements (of eq. 8), the following expression for the stream infiltration is obtained

$$C_r W_r \left(\frac{\Delta h}{1+\frac{C_r W_r (D+t_a+W_r/2)}{2K_a t_a}}\right) < Q_r < C_r W_r \left(\frac{\Delta h}{1+\frac{C_r W_r D}{2K_a t_a}}\right) \tag{10}$$

The Q_r thus obtained avoids the uncertainties associated with quantifying h_{int} as suggested in Cremeans & Devlin, (2017). Eq. (10) in contrast to eq. (1), seems to have a nonlinear relation of flux with streambed and aquifer parameters. This is in contrast to a widely used linear approach (e.g. RIV package). The nonlinear behaviour of the flux is explored in the next section.

3. Behaviour of the flux

The presented analytical approach (eq. 10) seems to behave non-linearly with respect to streambed and aquifer properties. The further analysis of the nonlinear behaviour is performed using the conceptualised model setup in Fig 1 with parameters - $W_a = 45\,m$, $W_r = 15\,m$, $\Delta h = 0.1\,m$, $K_a = 1E-4\ m/s$ and $t_a = 10\,m$. The specific conductance C_r being a critical parameter for direct quantification is used to compare the flux (Fig. 2). The $C_r$values are calculated by varying K_r ($1E-6\ m/s\ to\ 1E-4\,m/s$) and t_r ($0.01\,m\ to\ 0.75\,m$). Figure 2 represents the variation of flux with C_r. The curve appears to follow a logistic curve with both the extremus and thus clearly nonlinear. The flux tends to become constant after a certain value of C_r(1E-4 for the above-described setup), which restricts flux to a certain maximum depending

upon the hydraulic and geometrical properties of the streambed and the aquifer. However, in eq. (1), the flux increases by increasing the C_r. This indicates a large overestimation of flux obtained using eq. (1). Furthermore, from eqs. (1) and (10), the head difference corresponds to the slope of the two approaches, subject to the condition when specific conductance tends to 0. Owing to this condition, the overlap between the two curves is restricted to a very small region.

Limited by the availability of field and lab data, the study further extends to examine the nonlinear behaviour using the synthetic numerical experiment of the above-conceptualised setup.

3.1. Numerical example

An identical numerical domain is setup using the same model dimensions that were used as in section 3. Further, the model includes all the assumptions made above for the development of the concept presented in eq. (10). In the numerical domain, the Dirichlet boundary (left and right 0 and stream head = 0.1) is applied at the infiltrating stream and at the edge of the domain. The aquifer bottom in the setup is the no-flow boundary. The Gmsh mesh generator (Geuzaine & Remacle, 2017) was utilised for the finite element discretisation of the model domain, and an optimal mesh size was determined as smaller elements near the streambed (0.3) and larger near the aquifer boundaries (0.5). Scenarios were simulated using the open-source Groundwater_Flow module of numerical modelling tool OpenGeoSys v6.1 (www.opengeosys.org). The tool uses a linear homogeneous elliptic equation

$$div(k\ grad\ h) = 0 \text{ in } \Omega \tag{11}$$

with respect to boundary conditions

$$h(x) = g_D(x) \text{ on } \Gamma_D, \frac{k\partial h(x)}{\partial n} = g_{N(x)} \text{ on } \Gamma_N,$$

where h is the hydraulic head, D and N denote the Dirichlet- and Neumann-type boundary conditions $\boldsymbol{n}$ represent normal vector pointing outside of Ω, and $\Gamma = \Gamma_D \cup \Gamma_N$ and $\Gamma_D \cap \Gamma_N = \emptyset$ (further details can be obtained from:

https://www.opengeosys.org/docs/benchmarks/elliptic/elliptic-dirichlet/).

Figure 2 presents the results of numerical simulations. In the figure both the calculated and the simulated fluxes from different scenarios (varying K_r and t_r), are compared with respect to the specific conductance (C_r). As can be observed, the simulated results follow the same trend and lie between the calculated fluxes for both the limits resulting from eq. (10).

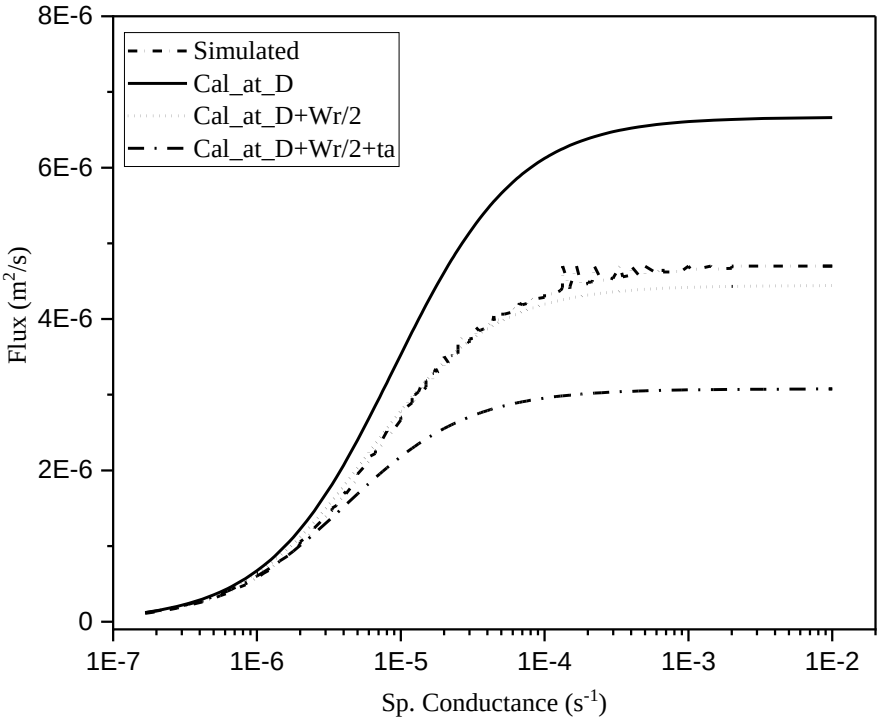

Figure 2: Comparison between the numerically obtained flux with that obtained using the developed analytical approach for three different streamlines.

Further, from eq. (7a) the simulated flux at any aquifer boundary will be half the magnitude of the calculated flux from eq. (10). The significant variation in the calculated flux magnitude is observed with the selection of the following three different distances: (1) at $D = (W_a - W_r)/2$; (2) at $D + t_a + W_r/2 = W_a/2 + t_a$ and (3) at $D + W_r/2 = W_a + W_r/2$ (Fig. 2). These three curves correspond to the effect of the gradients on the flux referring to the location of head measurements. The simulated curve is calculated at distance $D + W_r/2$, where $D < (W_a - W_r)/2$**,** and represents the case between cases 1 and 2 mentioned above. The distance in the simulated scenario is close to case 3, and hence the difference between the two curves is smaller than the curve for cases 1 and 2. The influence of hydraulic gradients is observed to be greater at higher specific conductance (>10^{-5} s^{-1}). On the other hand, all four curves have insignificant

differences in flux at lower specific conductance ($<10^{-6}$ s^{-1}). The fluxes are found to be reaching a maximum at higher specific conductance (10^{-3} s^{-1}). The calculated and the simulated curves agree with the nonlinear behaviour of the flux with respect to the conductance and hence contradicts the linear behaviour of the flux. The curves have minimum flux at a lower C_r value and maximum at a higher C_r value.

Beyond the maximum specific conductance, the system tends to be governed by the aquifer properties (see Fig. 2). The behaviour is in line with the physical system, i.e., where the conductance of streambed is greater than the aquifer hydraulic conductivity, the flux determined in the aquifer will be governed by the aquifer properties and not by the streambed conductance. This limits the application of eq. (1) where the flux is based only on the streambed properties. The developed approach hence can be considered as a more suitable approach towards the exchange estimation as compared to the conductance-based approach when aquifer properties are to be included as part of the model development. The value of the flux ranges between the mentioned two cases and also verifies the assumption made in eq. (3). This assumption holds true for different simulated scenarios (not presented in this work).

4. Significance of the approach

4.1 Significance of the aquifer properties

The developed approach in this work strongly emphasises on the incorporation of aquifer properties for the quantification of the exchange flux. Based on the discussion in the previous sections, the $h_{aquifer}$ is either measured beneath the stream bed or is replaced with h_{rbot}. If considering the field measurements of the head beneath the streambed, in an ideal case, the measurement should be done at the interface of the streambed bottom and the aquifer. However, due to uncertainties involved in the delineation of the streambed and its varying thickness, the head measurements are either in the streambed or at a certain depth in the aquifer. In the latter case, the measured head has an influence of both streambed and the aquifer. The hydraulic properties of the aquifer, as well as the geometry (mainly the thickness) of the aquifer, have a significant impact on the head drop between the streambed bottom and the point of measurement in the aquifer. This section illustrates the impact of these properties on the exchange quantification.

The proposed expression (eq. 10) includes the thickness and the hydraulic conductivity of the aquifer and the width of the streambed. The width of the aquifer, in the current study, represents the extent of the aquifer at which head and flux measurements are to be done (see Fig. 1). This section hence focuses on the influence of the thickness and the hydraulic conductivity of the aquifer. For the illustration, the aquifer thickness and the hydraulic conductivity with a different specific conductance of the streambed are varied, and obtained results are subsequently discussed.

4.1.1 Thickness of the aquifer

In a natural stream-aquifer system, the aquifer can be a shallow or a deep aquifer or within these two extremes. Considering eq. (10), the aquifer thickness defines the longest and the shortest streamlines for exchange quantification. These streamlines have a significant effect when the aquifer is shallow. To further illustrate the significance, eight specific conductance with minimum 1E-8 (s^{-1}) to maximum 1E-4 (s^{-1}) were chosen depending on the minimum and maximum for the value of K_r (between 1E-6 m/s and 1E-4 m/s) and t_r (between 0.01 m to 0.75 m).

Figures 3a and 3b represent the variation in the thickness over a minimum aquifer thickness to a maximum aquifer thickness. The different curves tend to attain a constant value at a small aquifer thickness for a given specific conductance. The two plots signify the incorporation of the term t_a on eq. (10). For the specific conductance in the range of 1E-6 s^{-1} to 1E-5 s^{-1}, shallow aquifer shows much variation in flux than the deeper ones. Hence, t_a should be part of the flux estimation process especially for the shallow aquifers.

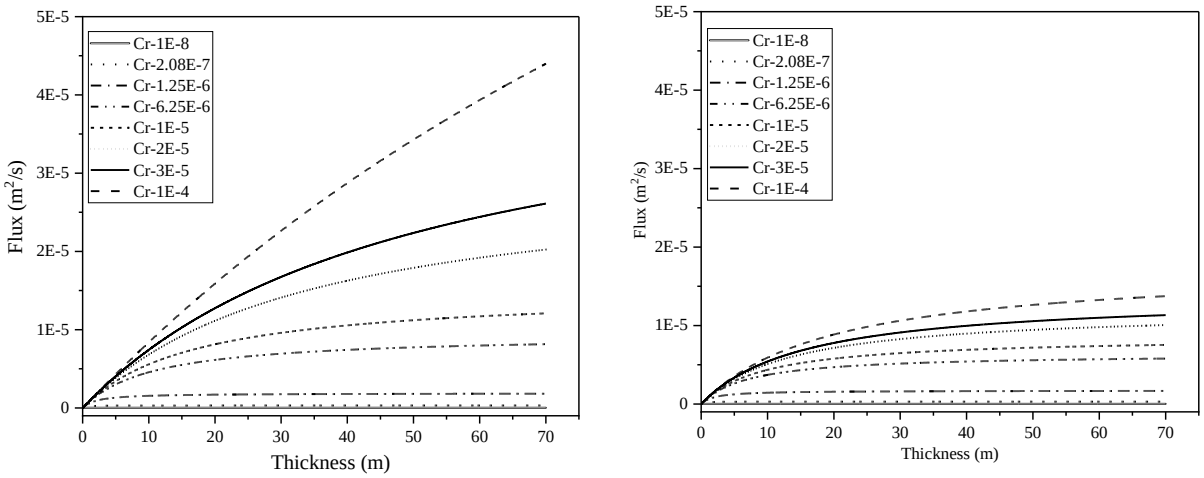

(a) (b)

Figure 3: Effect of aquifer thickness with varying specific conductance of the streambed at a (a) distance $D + W_r/2$ (b) distance $D + W_r/2 + t_a$.

4.1.2 Hydraulic Conductivity of aquifer

The hydraulic conductivity of the aquifer (K_a) is another quantity that can significantly influence the GW-SW flux estimation to illustrate this, analysis of eq. (10) is considered using the setup similar to that used for specific conductance analysis (see section 4.1.1).

Based on Fig. 3, $t_a = 15\,m$ was considered an appropriate aquifer thickness for analysing the effect of K_a on GW-SW flux. Figure 4 demonstrates the behaviour of the hydraulic conductivity of the aquifer on the interacting flux. The behaviour is very similar to the behaviour of thickness with varying specific conductance C_r. This implies that for a very small value of K_a flux is independent of the specific conductance and is only governed by the K_a (1E-6 m/s). However, for very high values of K_a (>1E-3 m/s), the flux becomes constant and is dependent only on the specific conductance of the streambed. This analysis provides the range of K_a and the dependency of the flux on that range.

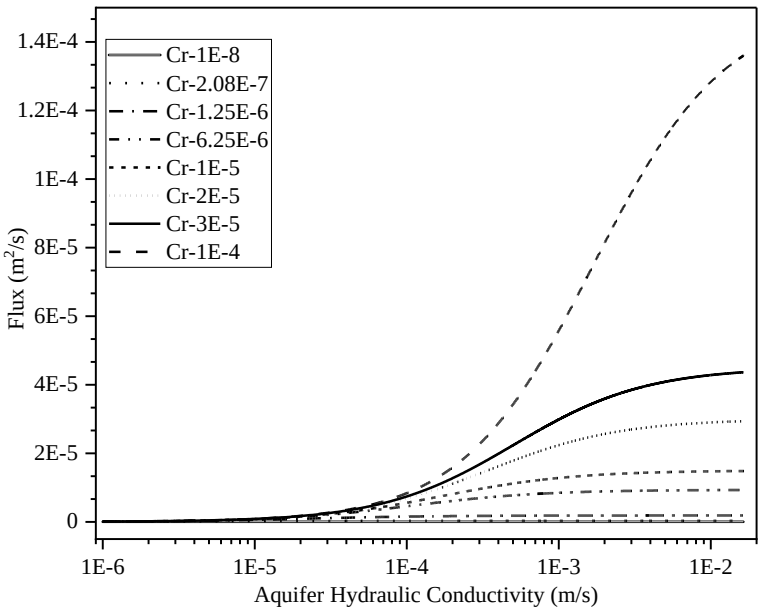

Figure 4: Effect of aquifer conductivity with varying specific conductance of the streambed

4.2 Determination of Specific Conductance C_r

Eq. (10) presents a straightforward method for the determination of GW-SW exchange flux. This approach can further be extended for the estimation of other streambed quantities. As already discussed, the conductance or the hydraulic conductivity of the streambed (C_r) is the most critical parameter in the determination of GW-SW exchanges. Also, in numerical modelling, estimating its magnitude is among the most challenging tasks. The details below utilise eq. (8) eq. (10) to provide an approach to easily obtain C_r.

First, eq. (8) is modified by replacing the value of K_r/t_r from eq. (10), as

$$\frac{1}{C_r W_r} < \frac{\Delta h}{Q_r} - \frac{D}{2K_a t_a} < \frac{\Delta h}{Q_r} - \frac{(D+t_a+W_r/2)}{2K_a t_a} \tag{12}$$

Rearranging the above equation provides the expression for C_r as

$$\frac{2K_a t_a Q_r}{W_r(\,2K_a t_a \Delta h - Q_r D)} < C_r < \frac{2K_a t_a Q_r}{W_r(\,2K_a t_a \Delta h - Q_r (D + t_a + W_r/2))} \quad (13)$$

Eq. (13) defines C_r from five quantities: the aquifer conductivity and thickness ($K_a t_a$), the width of the streambed (W_r), measured head (Δh), the distance of head measurement (D or $D + t_a + W_r/2$) and the infiltrating flux (Q_r). These parameters can be measured directly in the field or can be obtained using indirect estimation techniques.

For example, W_r can either be measured with a meter tape when the width is small or using remote sensing based on photogrammetry technology (Javernick et al., 2014). Ground-based cameras are another technique to measure the width (see Leduc et al., 2018). Aquifer properties such as transmissivity are most widely determined using the pumping tests. A slug test can be used for the quick estimate for the aquifer properties. Among these parameters, the most critical parameter in eq. (13) is Q_r and its determination is crucial for the estimation of C_r. The sub-section below presents an approach to quantify it.

Determination of Q_r

There are several techniques for the direct measurement of the infiltrating flux through the streambed, e.g. seepage meters (Rosenberry et al., 2020). In addition to the direct measurement techniques, there are several indirect techniques to quantify the exchanging flux. Among these, the flux estimation using heat as the tracer is most common (Gordon et al., 2012; Lautz et al., 2010).

The above-mentioned techniques consider measurements in the stream, which is subjected to challenges including streamflow, alteration of the streambed hydraulic conductivity due to instrument installation, and is limited to point measurement of the data. These challenges can be overcome if we could estimate the infiltrating flux in the surrounding aquifer.

The GW-SW interaction system, as also considered in this work, can be treated as a superimposed system of groundwater flow and the stream infiltration (see Section 2). Therefore, the flux estimated at any aquifer boundary, i.e. the point of measurements on both sides of the stream (say right side flux be - Q_{ar} and left side flux be - Q_{al}) will have the influence of both

306 groundwater flow in the aquifer (Q_a) and the stream infiltration (Q_r). In a losing stream, the
307 fluxes thus can be obtained from

$$Q_{al} = Q_a + Q_r/2 \tag{14a}$$

$$Q_{ar} = Q_a - Q_r/2 \tag{14b}$$

308 The Q_r in the eq. (14b) represents the opposite direction of contributing stream flux with respect
309 to the groundwater flow in the aquifer. Subtracting eq. (14 b) from eq. (14 a) provides the
310 following expression for Q_r:

$$Q_r = Q_{al} - Q_{ar} \tag{15}$$

311 The fluxes Q_{al} and Q_{ar}, can be estimated by measuring the head gradient on the left and the
312 right side of the stream (as shown in Fig. 1). This method involves measurement of the stream
313 stage and groundwater heads in a network of wells on both sides of the stream, to calculate
314 gradients and then the exchanging flux. The method is suitable when the groundwater flow is
315 lateral to the streamflow. However, the case of losing and gaining stream could be addressed
316 using this approach by simply changing the direction of the flow.

317 **5. Conclusions and Outlook**

318 The conductance-based approach, a linear approach, requires modification for determining the
319 stream-aquifer interaction. The approach involves challenges in the determination of hydraulic
320 head below the streambed and the conductance of the streambed. The developed formulation
321 provides a more logistic approach towards the determination of the GW-SW interaction by
322 eliminating the uncertainties and challenges involved in the head measurement required below
323 the streambed. This straightforward approach is extended for the development of the expression
324 for the streambed parameter estimation. The formulated expression for the streambed flux and
325 the streambed specific conductance holds for the different numerical simulations. These
326 numerically verified expressions can further be tested using field measurements/data. The

exchange flux could either be quantified using the head measurement in the aquifer or direct quantification of the flux using heat measurement techniques.

The GW-SW interaction is a very complex process, and hence a step-by-step model built up, and process understanding is very necessary. The presented approach involves many assumptions. However, the concept could be extended to address the more complex systems involving the asymmetric stream-aquifer system and varying the hydraulic head along the edge of the aquifer. In a natural stream-aquifer system, the orientation of the groundwater flow could be along the streamflow, lateral to the stream or flowing at some angle to the direction of streamflow. These issues could be addressed by extending to the 3-dimensional model.

Acknowledgements

The work was partially funded by Deutscher Akademischer Austauschdienst (DAAD) (*Research Grants – Bi-nationally Supervised Doctoral Degrees)*, and Ministry of Human Resources Development, India. The development of the presented work did not use any data, nor created any dataset. Parameter values and ranges have been used for the development of the curves and are already cited in the text above.

References

Alzraiee, A. H., Bailey, R., & Bau, D. (2017). Assimilation of historical head data to estimate spatial distributions of stream bed and aquifer hydraulic conductivity fields. *Hydrological Processes*, *31*(7), 1527–1538. https://doi.org/10.1002/hyp.11123

Bencala, K. E. (2005). Hyporheic exchange flows. *Encyclopedia of Hydrological Sciences*, (APRIL 2006), 1–7. https://doi.org/10.1002/0470848944.hsa126

Benoit, S., Ghysels, G., Gommers, K., Hermans, T., Nguyen, F., & Huysmans, M. (2019). Characterisation of spatially variable riverbed hydraulic conductivity using electrical resistivity tomography and induced polarisation. *Hydrogeology Journal*, *27*(1), 395–407. https://doi.org/10.1007/s10040-018-1862-7

Boano, F., Harvey, J. W., Marion, A., Packman, A. I., Revelli, R., Ridolfi, L., & Wörman, A. (2014). Hyporheic flow and transport processes: Mechanisms, models, and biogeochemical implications. *Reviews of Geophysics*, *52*(4), 603–679. https://doi.org/10.1002/2012RG000417

Boulton, A. J., Findlay, S., Marmonier, P., Stanley, E. H., & Valett, H. M. (1998). THE FUNCTIONAL SIGNIFICANCE OF THE HYPORHEIC ZONE IN STREAMS AND RIVERS. *Annu. Rev. Ecol. Syst*, *29*, 59–81.

Brunner, P., Simmons, C. T., Cook, P. G., & Therrien, R. (2010). Modeling surface water-groundwater interaction with MODFLOW: Some considerations. *Ground Water*, *48*(2), 174–180. https://doi.org/10.1111/j.1745-6584.2009.00644.x

Brunner, P., Therrien, R., Renard, P., Simmons, C. T., & Franssen, H. J. H. (2017). Advances in understanding river-groundwater interactions. *Reviews of Geophysics*, *55*(3), 818–854. https://doi.org/10.1002/2017RG000556

Cardenas, M. B., Wilson, J. L., & Zlotnik, V. A. (2004). Impact of heterogeneity, bed forms, and stream curvature on subchannel hyporheic exchange. *Water Resources Research*, *40*(8), 1–14. https://doi.org/10.1029/2004WR003008

Cousquer, Y., Pryet, A., Flipo, N., Delbart, C., & Dupuy, A. (2017). Estimating River Conductance from Prior Information to Improve Surface-Subsurface Model Calibration. *Groundwater*, *55*(3), 408–418. https://doi.org/10.1111/gwat.12492

Cremeans, M. M., & Devlin, J. F. (2017). Validation of a new device to quantify groundwater-surface water exchange. *Journal of Contaminant Hydrology*, *206*, 75–80. https://doi.org/10.1016/j.jconhyd.2017.08.005

Frei, S., Fleckenstein, J. H., Kollet, S. J., & Maxwell, R. M. (2009). Patterns and dynamics of river-aquifer exchange with variably-saturated flow using a fully-coupled model. *Journal of Hydrology*, *375*(3–4), 383–393. https://doi.org/10.1016/j.jhydrol.2009.06.038

Geuzaine, C., & Remacle, J.-F. (2017). A three-dimensional finite element mesh generator with built-in pre- and post-processing facilities. *Int. J. Numer. Meth. Engng.*, *79*(11), 1309–1331. Retrieved from http://gmsh.info//doc/preprints/gmsh_paper_preprint.pdf

Ghysels, G., Mutua, S., Veliz, G. B., & Huysmans, M. (2019). A modified approach for modelling river–aquifer interaction of gaining rivers in MODFLOW, including riverbed heterogeneity and river bank seepage. *Hydrogeology Journal*, 1–13. https://doi.org/10.1007/s10040-019-01941-0

Gooseff, M. N., Anderson, J. K., Wondzell, S. M., LaNier, J., & Haggerty, R. (2006). A modelling study of hyporheic exchange pattern and the sequence, size, and spacing of stream bedforms in mountain stream networks, Oregon, USA. *Hydrological Processes*. https://doi.org/10.1002/hyp.6349

Gordon, R. P., Lautz, L. K., Briggs, M. A., & McKenzie, J. M. (2012). Automated calculation of vertical pore-water flux from field temperature time series using the VFLUX method and computer program. *Journal of Hydrology*, *420–421*, 142–158. https://doi.org/10.1016/j.jhydrol.2011.11.053

Kalbus, E., Schmidt, C., Molson, J. W., Reinstorf, F., & Schirmer, M. (2009). Influence of aquifer and streambed heterogeneity on the distribution of groundwater discharge. *Hydrology and Earth System Sciences*, *13*(1), 69–77. https://doi.org/10.5194/hess-13-69-

2009

Lautz, L. K., Kranes, N. T., & Siegel, D. I. (2010). Heat tracing of heterogeneous hyporheic exchange adjacent to in-stream geomorphic features. *Hydrological Processes*, *24*(21), 3074–3086. https://doi.org/10.1002/hyp.7723

Leduc, P., Ashmore, P., & Sjogren, D. (2018). Technical note: Stage and water width measurement of a mountain stream using a simple time-lapse camera. *Hydrology and Earth System Sciences*, *22*(1), 1–11. https://doi.org/10.5194/hess-22-1-2018

Malard, F., Tockner, K., Dole-Olivier, M.-J., & Ward, J. V. (2002). A landscape perspective of surface-subsurface hydrological exchanges in river corridors. *Freshwater Biology*, *47*(4), 621–640. https://doi.org/10.1046/j.1365-2427.2002.00906.x

McDonald, M. G., & Harbaugh, A. W. (1988). *A modular three-dimensional finite-difference ground-water flow model*. *Techniques of Water-Resources Investigations*. https://doi.org/10.3133/twri06A1

McLachlan, P. J., Chambers, J. E., Uhlemann, S. S., & Binley, A. (2017). Geophysical characterisation of the groundwater–surface water interface. *Advances in Water Resources*, *109*, 302–319. https://doi.org/10.1016/j.advwatres.2017.09.016

Rosenberry, D. O., Duque, C., & Lee, D. R. (2020, May 1). History and evolution of seepage meters for quantifying flow between groundwater and surface water: Part 1 – Freshwater settings. *Earth-Science Reviews*. Elsevier B.V. https://doi.org/10.1016/j.earscirev.2020.103167

Tang, Q., Kurtz, W., Schilling, O. S., Brunner, P., Vereecken, H., & Hendricks Franssen, H. J. (2017). The influence of riverbed heterogeneity patterns on river-aquifer exchange fluxes under different connection regimes. *Journal of Hydrology*, *554*, 383–396. https://doi.org/10.1016/j.jhydrol.2017.09.031

Vogt, T., Schneider, P., Hahn-Woernle, L., & Cirpka, O. A. (2010). Estimation of seepage rates in a losing stream by means of fiber-optic high-resolution vertical temperature profiling. *Journal of Hydrology*, *380*(1–2), 154–164. https://doi.org/10.1016/j.jhydrol.2009.10.033